MACHINED SURFACE ROUGHNESS INCLUDING CUTTER DISPLACEMENTS IN MILLING OF HARDENED STEEL

Szymon Wojciechowski

Poznan University of Technology, Faculty of Mechanical Engineering, ul. Piotrowo 3, 60-965 Poznan, Poland (✉sjwojciechowski@o2.pl)

Abstract

The work presented here, concentrates on experimental surface roughness analysis in the milling of hardened steel using a monolithic torus mill. Machined surface roughness with respect to milling process dynamics has been investigated. The surface roughness model including cutter displacements has been developed. Cutting forces and cutter displacements (vibrations) were measured in order to estimate their quantitative influence on Ra and Rz parameters. The cutter displacements were measured online using a scanning 3D laser vibrometer. The influence of cutting speed v_c on surface roughness parameters (Ra, Rz) was also studied. The research revealed that real surface roughness parameters are significantly higher than those calculated on the basis of a kinematic-geometric basic model, and their values are strongly dependent on dynamic cutter displacements.

Keywords: milling, surface roughness, dynamics, hardened steel, scanning vibrometry

1. Introduction

Surface roughness is one of the most important factors determining machined surface quality, and thereupon its accurate estimation is the subject of a lot of research [1, 2]. According to the kinematic-geometric projection of the cutter into the work piece, one of the most influential factors on machined surface roughness is feed per tooth f_z. Many researchers report that an increase in feed per tooth f_z induces surface roughness growth after end milling in HSM conditions [3-6].

Nonetheless, on the basis of several works related to the machining of hardened steel [7, 8] and tungsten carbide [9], the dominant factor affecting surface micro-irregularities is not feed per tooth f_z, but feed per revolution f, which is directly related to cutter radial run-out and rotational speed n which affects centrifugal force. Feed (f, f_z,) cutting speed v_c [10-12], axial and radial depth of cut (a_p, a_e) determine dominant factors in HSM process prognostic model elaboration [13-16].

According to research [7, 8] related to the milling of hardened steel 55NiCrMoV6, it can be seen that real surface roughness parameters are from 15 to 20 times higher than theoretical values resulting from kinematic-geometric projection. The displacements of the working parts of the cutter (vibrations) are the main reason for these discrepancies. The above-mentioned displacements are caused by various conditions. Thus, in the discussion of the most important factors affecting machined surface roughness, it is necessary to include the effect of vibrations [17-23]. Several works [24-27] are related to surface texture modeling (primarily surface location error SLE and surface roughness) in the range of chatter occurrence (range of non-stability). From the practical point of view, the estimation of surface roughness in a stable process is essential, since in industry it is necessary to avoid the chatter. According to research [28, 29] one of the most significant conditions affecting machined surface roughness in a stable process is the cutter's radial run-out. This phenomenon is caused either by tool axis

www.czasopisma.pan.pl PAN www.journals.pan.pl

POLSKA AKADEMIA NAUK

S. Wojciechowski: MACHINED SURFACE ROUGHNESS INCLUDING CUTTER DISPLACEMENTS IN MILLING OF ...

tilt or displacement with reference to spindle axis. Furthermore in the range of high rotational speeds, which induces high centrifugal force, the cutter's radial run-out can be multiplied, which in turn affects machined surface roughness.

In this paper, the surface roughness model including cutter displacements have been adopted from the previous study [1] and extended for milling tools with varying numbers of teeth z. Cutter displacements were calculated on the basis of instantaneous maximal force alterations substituted into the differential motion equation. These calculated displacement values were compared to those measured using a 3D scanning laser vibrometer.

2. Surface roughness modeling in cylindrical milling process

According to the kinematic-geometric projection of the cutter into the work piece, theoretical surface roughness height in the cylindrical milling process can be formulated by the following equation [3]:

$$Rt_0 = \frac{D}{2} - \sqrt{\frac{D^2 - f_z^2}{4}} \approx \frac{f_z^2}{4 \cdot D},$$ (1)

where: Rt_0 – theoretical surface roughness, f_z – feed per tooth, D – tool diameter.

From formula (1) it can be clearly seen that an increase in feed per tooth f_z causes surface roughness growth, whereas an increase in tool diameter D causes a decline in surface roughness. However, theoretical models describing alterations of surface roughness parameters in the function of kinematic-geometric parameters often vary from the real surface roughness value, especially for low feed values. During the generation of surface irregularities in the finishing process in HSM conditions, process dynamics (*e.g.* related to the cutter's radial run-out) has significant meaning. Figure 1 depicts the projection of the cutter into the work piece, including the cutter's displacement induced by the cutter's radial run-out.

a) for tool with number of teeth $z = 2$.
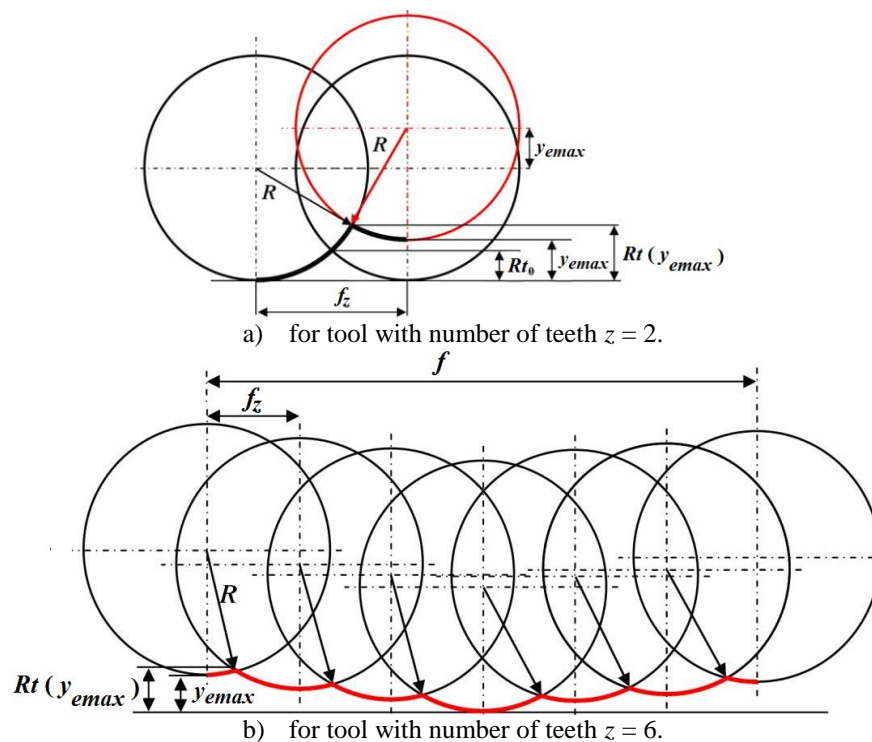
b) for tool with number of teeth $z = 6$.

Fig. 1. Projection of the cutter into the work piece including cutter displacement, where: R – tool radius, f – feed per revolution, f_z – feed per tooth, y_{emax} – maximum value of cutter displacement envelope, $Rt(y_{emax})$ – surface roughness height including cutter displacement, Rt_0 – theoretical surface roughness.

www.czasopisma.pan.pl   PAN   www.journals.pan.pl
POLSKA AKADEMIA NAUK

Metrol. Meas. Syst., Vol. XVIII, (2011), No. 3, pp. 429-440.

Cutter run-out can be due to the tool itself (wear, asymmetry, insert setting, dynamic imbalance and thermal deformation) but it is mainly due to the offset between the position of the tool rotation axis and the spindle rotation axis. The consequence is a tool rotation around the spindle axis with an eccentricity which induces cutter displacement $y_{e\max}$. These displacements relocate directly on the work piece (along the closed trajectory in *X-Y* plane), generating surface roughness (see Fig. 1). Moreover, $y_{e\max}$ values can be also affected by cutting forces and, at higher rotational speeds *n,* by centrifugal forces.

The model depicted in Fig. 1 is related to the case when the tool rotates around the spindle axis with an eccentricity and the cutter's displacement $y_{e\max}$ is significantly lower than the tool radius *R*, $y_{e\max} << R$, as well as the radial depth of cut a_e, $y_{e\max} << a_e$. For simplification it was assumed that teeth location errors were neglected, which means that partial displacements for consecutive teeth are uniform. It is necessary to emphasize that this assumption can be valid only for monolithic tools. In the case of inserted tools, the influence of insert setting error must be included. The developed model is not taking into account the problem of minimum uncut chip thickness h_{min}, which can have an influence on the generated surface roughness, especially in machining with low sectional areas of cut. Nevertheless in the machining of hardened steels h_{min} values are very low and thus their influence can be neglected. From Fig. 1 it can be seen that the higher the displacements $y_{e\max}$ (vibrations), the greater the surface micro-irregularities values, and consequently surface roughness parameters (*e.g.* $Rt(y_{e\max})$). On the basis of the dependencies depicted in Fig. 1, surface roughness height including cutter displacement $Rt(y_{e\max})$ can be formulated as:

$$Rt(y_{e\max}) = \frac{2\left(4 y_{e\max}^2 + f_z^2 \cdot z^2\right)\cdot\left(y_{e\max}\cdot z\right) - f_z \cdot z \cdot \sqrt{4 y_{e\max}^2 + f_z^2 \cdot z^2}\cdot\sqrt{z^2\left(4R^2 - f_z^2\right) - 4 y_{e\max}^2}}{2z\cdot\left(4 y_{e\max}^2 + f_z^2 \cdot z^2\right)} -$$
$$-\frac{2\left(4 y_{e\max}^3 - 4R\cdot y_{e\max}^2 \cdot z + f_z^2 \cdot y_{e\max}\cdot z^2 - f_z^2 \cdot R \cdot z^3\right)}{2z\cdot\left(4 y_{e\max}^2 + f_z^2 \cdot z^2\right)}, \tag{2}$$

where: $Rt(y_{e\max})$ – surface roughness height including cutter displacement, $y_{e\max}$ – maximum value of cutter displacement envelope, z – number of teeth.

Formula (2) was developed on the basis of trigonometric dependencies presented in Fig. 1, between feed per tooth f_z, cutter radius *R*, displacement $y_{e\max}$, number of teeth *z* and surface roughness height $Rt(y_{e\max})$. In order to simplify the algebraic transformations, Derive 6 software was applied. This equation is valid only for an even number of teeth and when $z \geq 2$. When cutter displacement $y_{e\max}$ is equal to zero, formula (2) simplifies to (1). The average surface roughness parameter including cutter displacement $Ra(y_{e\max})$ can be calculated from the following equation:

$$Ra(y_{e\max}) = -\frac{3\cdot Rt(y_{e\max})\left(3\cdot Rt(y_{e\max}) + 4\cdot R\right)\cdot\left(3\cdot Rt(y_{e\max})^2 + 4\cdot Rt(y_{e\max})\cdot R - 20\cdot R^2\right)}{1000\cdot R^3}. \tag{3}$$

Formula (3) was developed on the assumption that the average surface roughness value is equal to the mean arithmetic deviation of profile line from the average line. The surface irregularity profile line is marked on Fig. 1 by the thick black line. In order to determine the average line of surface irregularity profile, the center of gravity of area below the profile was calculated. The Derive 6 software was applied once again to simplify the calculations.

The unknown quantity in formulas (2) and (3) is displacement $y_{e\max}$. In order to calculate total displacement of the cutter *y* which includes displacement induced by cutting forces y_F and displacement caused by dynamic run-out y_e (so-called cutter displacement envelope) it is necessary to solve the differential motion equation:

www.czasopisma.pan.pl PAN www.journals.pan.pl

POLSKA AKADEMIA NAUK

S. Wojciechowski: MACHINED SURFACE ROUGHNESS INCLUDING CUTTER DISPLACEMENTS IN MILLING OF ...

$$m \cdot \ddot{y}(t) + c \cdot \dot{y}(t) + k \cdot y(t) = F_{i\Delta e}(t). \tag{4}$$

In the first step, the left side of formula (4) was identified, *i.e.* modal parameters (m, c, k − for F_x and F_y directions) were determined using an impact test, and thus the following parameters were received [7, 8]: $m_x = 0,021$ Ns^2/m, $m_y = 0,019$ Ns^2/m, $c_x = 57$ Ns/m, $c_y = 45$ Ns/m, $k_x = 10172940$ N/m, $k_y = 8481764$ N/m. It is worth indicating that the determined values of modal parameters are valid only for a particular machine-collet-tool system. In order to define the right side of the equation (dynamic force $F_{i\Delta e}(t)$) it was assumed that cutter displacements are consequences of cutting forces and radial run-out which has an influence on maximal force amplitudes for consecutive teeth.

In the mechanistic force model for a cylindrical milling tool with non-zero helix angle ($\lambda_s > 0$), the cutting force F_c and cutting normal force F_{cN} are proportional to active sectional area of cut $A_z(\varphi)$ and specific cutting pressures(k_c, k_{cN}):

$$F_c = k_c \cdot A_z(\varphi), \tag{5}$$

$$F_{cN} = k_{cN} \cdot A_z(\varphi). \tag{6}$$

The F_f feed force and F_{fN} normal feed force components can be calculated on the basis of F_c and F_{cN} values and instantaneous rotation angle of cutting edge value φ:

$$F_f = \sum_{i=1}^{z_c} \left(F_{ci} \cos \varphi_i - F_{cNi} \sin \varphi_i \right), \tag{7}$$

$$F_{fN} = \sum_{i=1}^{z_c} \left(F_{ci} \sin \varphi_i + F_{cNi} \cos \varphi_i \right). \tag{8}$$

The method for the determination of cutting forces is described in [8], from which specific cutting pressure k_c, k_{cN} equations in function of uncut chip thickness per tooth h_z were selected as: $k_c = 4869,5\, h_z^{-0,34}$ [MPa] and $k_{cN} = 0,0003\, h_z^{-3,5}$[MPa].

The milling process, especially in HSM conditions, is accompanied by cutter radial run-out. The radial run-out during the milling process causes F_f and F_{fN} maximal force variation between each tooth. It is a cyclic phenomenon and force variation per tooth is a sine function (Fig. 2). With the purpose of taking into consideration the force variation per tooth, a new Δe_i constituent including tool radial run-out was introduced. In this relationship Δe_i constituent was developed based on the harmonic motion equation without damping. In F_f feed and F_{fN} normal feed force direction, the following equations are valid:

$$\Delta e_f = \left(\frac{k_{dFf} - 1}{2k_{dFf}} \right) \cdot \sin \left(\frac{\pi \cdot n \cdot t}{30} + \frac{\pi}{2} \right) + \left(\frac{k_{dFf} + 1}{2k_{dFf}} \right), \tag{9}$$

$$\Delta e_{fN} = \left(\frac{k_{dFfN} - 1}{2k_{dFfN}} \right) \cdot \sin \left(\frac{\pi \cdot n \cdot t}{30} + \frac{\pi}{2} \right) + \left(\frac{k_{dFfN} + 1}{2k_{dFfN}} \right), \tag{10}$$

where: k_{dFf}, k_{dFfN} − dynamics coefficient empirically determined.

Fig. 2 depicts the method for the determination of the dynamics coefficient k_d, in the F_{fN} time course when cylindrical milling with a 6-toothed milling cutter occurs. The dynamics coefficient k_d can be expressed by the following equation (where i denotes the direction of operating force: F_{fN}, F_f):

www.czasopisma.pan.pl PAN www.journals.pan.pl
POLSKA AKADEMIA NAUK

Metrol. Meas. Syst., Vol. XVIII, (2011), No. 3, pp. 429-440.

$$k_{di} = \left| \frac{F_i(y_{e\max})}{F_i(y_{e\min})} \right|, \tag{11}$$

where: $F_i(y_{e\max})$, $F_i(y_{e\min})$ – instantaneous force corresponding to maximum and minimum cutter displacement envelope value.
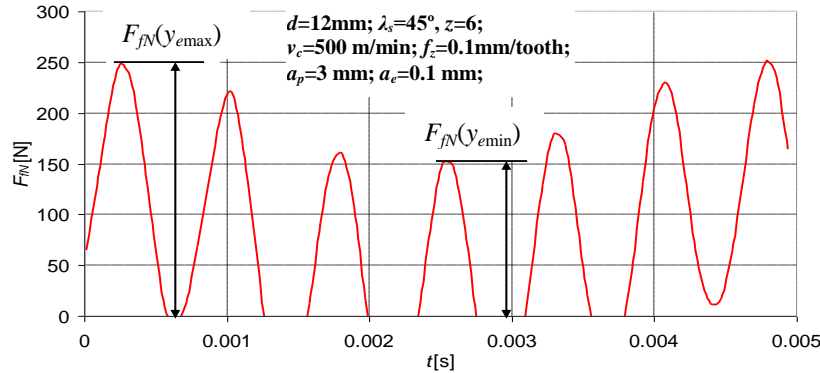

Fig. 2. The experimental time course of F_{fN} normal feed force component with the designation of instantaneous force corresponding to maximum $F_{fN}(y_{e\max})$ and minimum $F_{fN}(y_{e\min})$ cutter displacement envelope.

Empirically determined k_d values from formula (11) for various cutting speed v_c values can be expressed as a linear regression equation $k_d = f(v_c)$. Finally, equations of feed and normal feed force components including radial run-out of the cylindrical mill can be formulated as:

$$F_{f\Delta e} = \Delta e_f \cdot F_f, \tag{12}$$

$$F_{fN\Delta e} = \Delta e_f \cdot F_{fN}. \tag{13}$$

Determined values of dynamic force $F_{i\Delta e}(t)$ were substituted into formula (4), which was solved using a 4-th order Runge-Kutta algorithm in MatLab software. Displacements in feed direction (originated from the F_f component) were neglected because of their marginal influence on the generation of surface roughness parameters (Ra, Rz). After the calculations, total cutter displacements in the direction perpendicular to the machined surface y were obtained. In order to determine instantaneous values of cutter displacement envelope y_e, one should transform the right side of formula (4). In the proposed model it is assumed that cutter displacement envelope y_e is induced by the envelope of feed normal force $F_{fN\Delta e}(t)$. This force envelope $F_{fNe}(t)$ is defined as the difference between the instantaneous normal feed force including radial run-out $F_{fN\Delta e}(t)$ and the instantaneous force corresponding to minimum cutter displacement envelope $F_i(y_{e\min})$:

$$F_{fNe}(t) = F_{fN\Delta e}(t) - F_{fN}(y_{e\min}) = F_{fN\Delta e}(t) - \frac{F_{fN}(t)}{k_{dFfN}}. \tag{14}$$

After the substitution of formula (14) into formula (4), the cutter displacement envelope y_e can be obtained:

$$m \cdot \ddot{y}_e(t) + c \cdot \dot{y}_e(t) + k \cdot y_e(t) = F_{fNe}(t). \tag{15}$$

Subsequently maximum values of cutter displacement envelope $y_{e\max}$ obtained on the base of formula (15) were substituted into formulas (2) and (3).

3. Experimental details

3.1. Research range and method

In order to verify the proposed model a few series of milling tests with variable cutting conditions were performed. The investigations have been carried out on hardened hot-work tool steel coupons (55NiCrMoV6, hardness approx. 55 HRC). The monolithic torus mill ($z = 6$ number of teeth, $D = 12$ mm diameter, $r_\varepsilon = 1$ mm corner radius, $\lambda_s = 45°$ tool major cutting edge inclination angle, $r_n = 10$ µm radius of tool arc cutting edge) was selected as a milling cutter (Fig. 3a). The cutting edges were made from fine-grained sintered carbide (mean grain size approx. 0.4 µm) within TiAlCN anti-wear resistance coating. Experiments were conducted in free, down milling conditions, on 5-axes CNC milling workstation (DECKEL MAHO Co., model DMU 60monoBLOCK, see – Fig. 3b). Cutting parameters applied in the research are presented in Table 1.
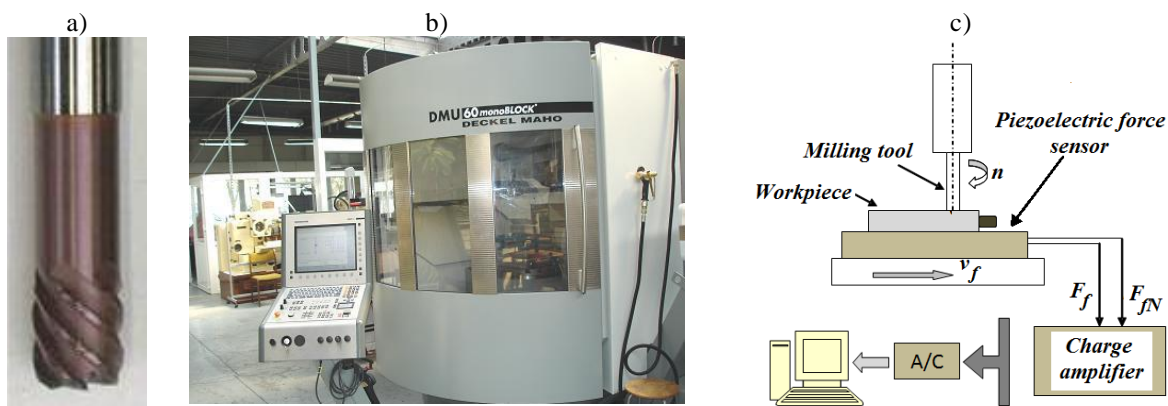

Fig. 3. Milling process experimental stand: a) the view of the employed tool; b) the view of DMG model DMU 60monoBLOCK milling center; c) block scheme of cutting force experimental apparatus.

In the research carried out, surface roughness parameters, cutting force components and tool displacements were measured for various cutting speed v_c values. In all investigated instances, the active number of teeth z_c was less than unity and tool wear per tooth was $VB_B < 0.05$ mm. Surface roughness measurements were made using a T500 portable surface profilometer (Hommelwerke), equipped with T5E head and Turbo DATAWIN software. A sampling length $lr = 0.8$ mm, the evaluation length $ln = 5 \cdot lr = 4.0$ mm, the length of cutoff wave $\lambda c = 0.8$ mm and an ISO 11562(M1) filter were applied.

Table 1. Cutting parameters applied in the research.

v_c [m/min]	f_z [mm/tooth]	v_f [mm/min]	a_p [mm]	a_e [mm]
100		1592		
200		3185		
300	0.1	4777	3	0.2
400		6370		
500		7962		

As a result of 2D measurements, surface profile charts were received. On the basis of surface profile charts, *Ra* and *Rz* parameters (according to ISO 4287:1984) were calculated using Turbo DATAWIN software. The measurement for each investigated cutting speed value was repeated 3 times in order to calculate the mean arithmetic value and range of *Ra* and *Rz* parameters. Parallel to surface roughness measurements, cutting force components were measured (in machine tool coordinates – Fig. 3c), in the following directions:

     –   dir. X – feed force F_f [N],
     –   dir. Y – feed normal force F_{fN} [N].

In order to verify cutter displacement values obtained from equation (4), appropriate measurements of cutter displacement were made. The scanning laser vibrometer Polytec PSV-400 was applied for measurements during the milling process (online). The measurements were made for three cutting speeds: v_c = 100, 200, 300 m/min. The diagram depicting displacement measurement is shown in Fig. 4a. Fig. 4b shows a view of the laser head during the calibration process. 3D cutter displacement measurements were conducted in the joining part of the $L2$ tool. For obvious reasons it is impossible to conduct the measurement on the working part of the tool during milling. In order to determine the displacement values on the working part of the tool (Fig. 4c, length $L1$) it is necessary to approximate displacement values on the joining part $\Delta e2$ to $\Delta e1$ values, assuming that the influence of L on Δe is described by the following equation:

$$\Delta e = \frac{F \cdot L^3}{3 \mathrm{E} I},$$
(16)

where: F – force acting on the tool, L – tool overhang, E – Young`s modulus, I – moment of inertia.

As a result of the 3D scanning laser vibrometer measurement, the time courses of instantaneous total cutter displacement y=f(t) values were obtained. On the basis of these y=f(t) courses, the mean arithmetic values, the range of maximum instantaneous displacements y per tooth as well as the maximum instantaneous displacement envelope $y_{e\max}$ per revolution were calculated.
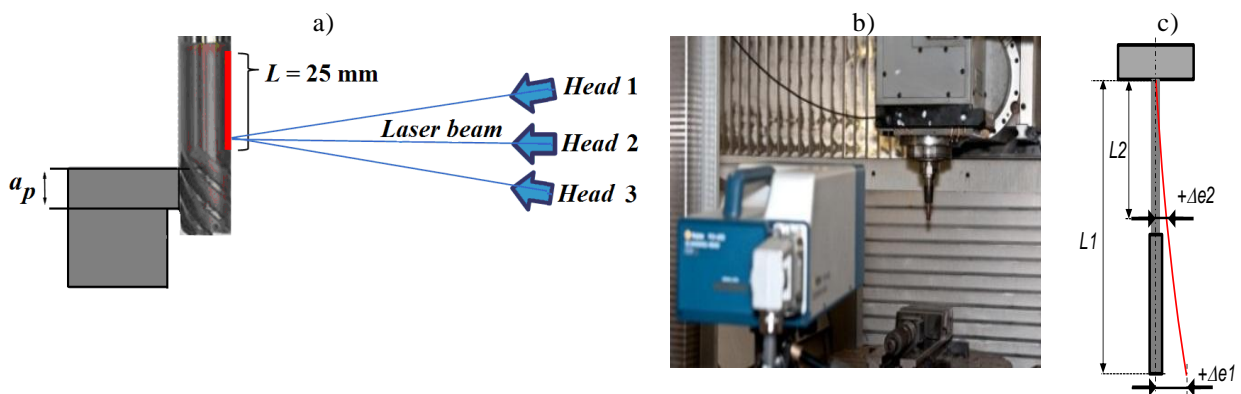

Fig. 4. Tool displacement measurement diagram: a) block scheme of 3D displacement measurement carried out on a scanning vibrometer; b) the view of laser head (no. 1) during the calibration process; c) the scheme of cutter displacement.

3.2. Experimental results and analysis

In Fig. 5a the time course for the feed normal component F_{fN} =f(t) for cutting speed v_c = 300 m/min is presented. Fig. 5b depicts the dynamics coefficient for feed normal component k_{dFfN} in the function of cutting speed v_c. It was found (Fig. 5a) that maximal instantaneous force F_{fN} values per consecutive tooth are not uniform. Alterations of these instantaneous maximal forces produce the envelope (thick black line), which has a period equal to tool revolution time. This is probably caused by the cutter's radial run-out phenomenon, related directly to the tool revolution period. Similar dependencies were observed for all remaining cutting speeds v_c. Fig. 5b shows that cutting speed growth causes a gentle increase of the dynamics coefficient, namely an amplitude growth of the force envelope (F_{fN}). This means

www.czasopisma.pan.pl   PAN   www.journals.pan.pl
POLSKA AKADEMIA NAUK

S. Wojciechowski: MACHINED SURFACE ROUGHNESS INCLUDING CUTTER DISPLACEMENTS IN MILLING OF ...

that the cutter's radial run-out value is multiplied by the tool displacements caused by centrifugal forces (related to cutting speed growth). Nonetheless, in the investigated cutting speed range v_c, the growth of the dynamics coefficient k_{dFfN} values are small (from 1,56 to 1,68).

In Fig. 6a the surface profile chart for cutting speed $v_c = 300$ m/min is presented. Fig. 6b depicts the surface profile chart with the superimposition of the F_{fN} force envelope for cutting speed $v_c = 300$ m/min. From Fig. 6a it can be seen that the surface micro-irregularities wavelength is 0.6 mm, which corresponds to a feed per revolution value ($f = z \cdot f_z = 6 \cdot 0.1 = 0.6$ mm/rev). Similar dependencies were observed for surface profiles generated for all the remaining cutting speeds v_c.
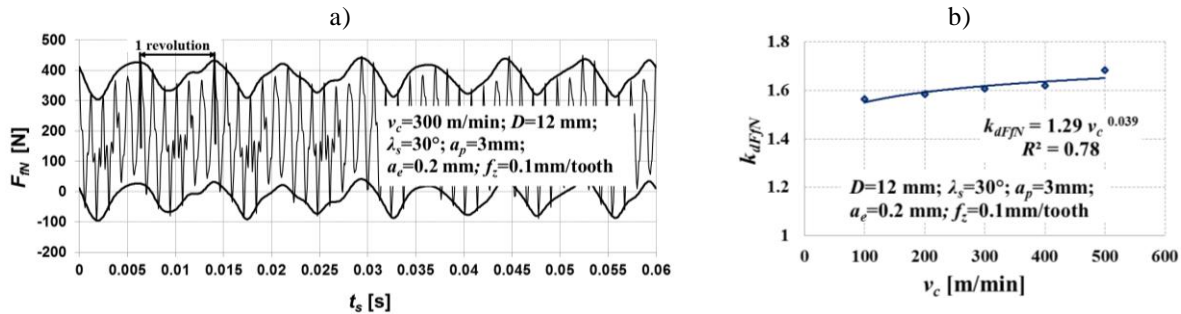

Fig. 5. a) time course for feed normal force component F_{fN} (thick black line denotes the envelope of F_{fN} force); b) dynamics coefficient k_{dFfN} in function of cutting speed v_c.
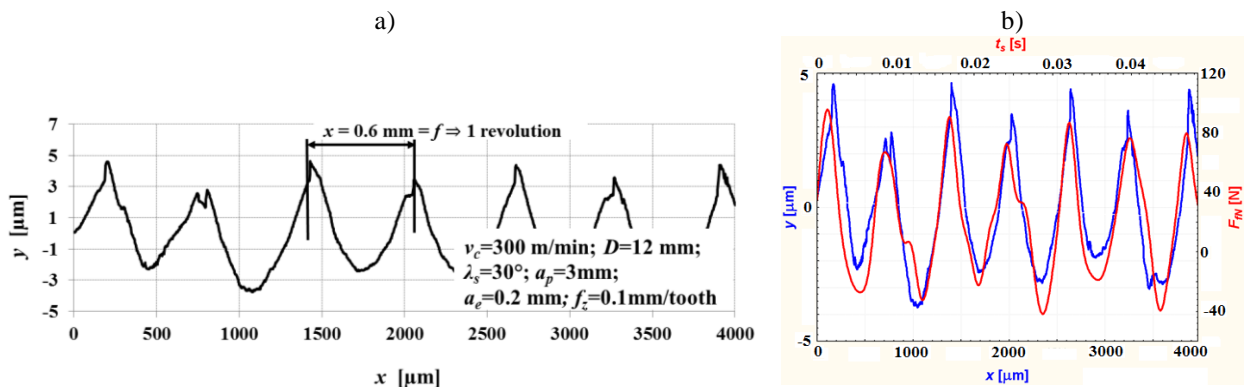

Fig. 6. a) surface profile chart; b) surface profile chart (blue line) with superimposed envelope of F_{fN} force (red line) for $v_c= 300$ m/min.

This dependence is inconsistent with the traditional kinematic-geometric projection of the cutter into the work piece expressed by formula (1). This formula assumes that the surface micro-irregularities wavelength is equal to the feed per tooth f_z value. Significant divergences are also found with reference to surface roughness height. According to formula (1), the theoretic height of surface roughness Rt_0 is equal to 0.21 μm, while the real surface roughness Rz value is significantly higher, with a value of $3.4 \div 7$ μm. Fig. 6b shows that some qualitative similarities can be found between the time course of the F_{fN} force envelope and the shape of the surface profile chart. This means that there is a clear relation between the instantaneous maximal force alterations and the generated surface profile. Based on foregoing observations one can indicate that the dominant factor influencing the machined surface profile is radial run-out related directly to the tool revolution period (and hence to feed per revolution f value).

Fig. 7a depicts the time course of total tool working part displacement $y=f(t)$, measured using a laser vibrometer with a cutting speed v_c of 300 m/min. Fig. 7b shows the time course of the envelope of cutter displacement $y_e=f(t)$, calculated in MatLab software (based on

www.czasopisma.pan.pl   PAN   www.journals.pan.pl
POLSKA AKADEMIA NAUK

Metrol. Meas. Syst., Vol. XVIII, (2011), No. 3, pp. 429-440.

equation (15)) for a cutting speed $v_c = 300$ m/min. It was found that (Fig. 7a) the cutter displacement wavelength is connected with the feed per tooth value f_z. This kind of displacement which has a frequency corresponding to the $z \cdot f_o$ (number of teeth multiplied by spindle rotational frequency) is caused by cutting forces (F_c, F_{cN},) generated in the milling process, that in turn cause displacements of each tooth. It is worth indicating that the above-mentioned displacements affect the surface location error – SLE. From Fig. 7a it can be also seen that maximal instantaneous displacement y values per consecutive teeth are not uniform. Alterations of these instantaneous maximal displacements produce the envelope (thick red line), which has a period equal to the tool revolution time. The shape of this envelope is similar to the sine course (however to a lesser extent than for the force envelope). The displacement envelope (y_e) is induced by cutter radial run-out.
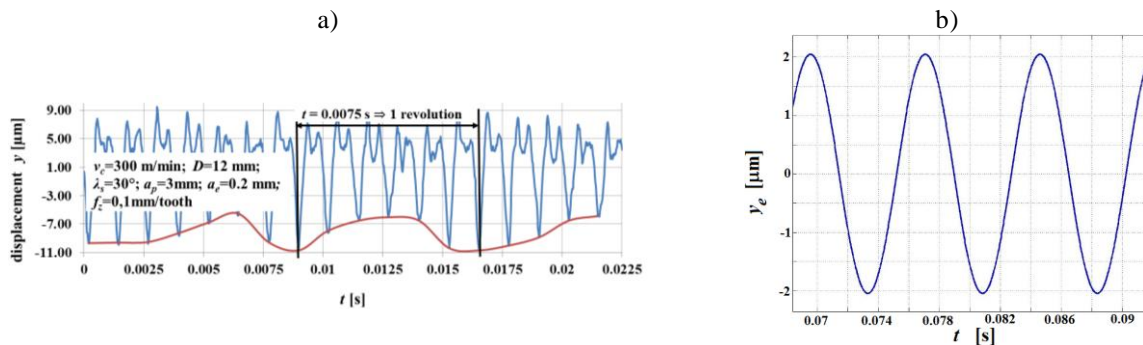
a)   b)

Fig. 7. a) the time course of measured total cutter displacement y (red line denotes the envelope of displacement y_e) for v_c= 300 m/min; b) the time course of simulated envelope of cutter displacement y_e for v_c= 300 m/min.

The maximal height of the envelope (equal to double of its amplitude) has a direct influence on force oscillations per tooth as well as machined surface roughness. The maximal height of the envelope measured by the vibrometer is equal to 4÷6 µm (Fig. 7a). This range of displacements stays in agreement with the real surface roughness height range for cutting speed $v_c = 300$ m/min (see – Fig. 6). From Fig. 7b it can be seen that the maximal height of the envelope calculated in MatLab software is equal to $y_{e\max}$= 4 µm. It stays in agreement with the range of values measured by the vibrometer (Fig. 7a).

Fig. 8 depicts the maximum instantaneous displacement envelope $y_{e\max}$ per tool revolution as well as the maximum instantaneous total displacement $y_{\max}$ per tooth in the cutting speed v_c function. Fig. 8a shows that mean arithmetic values of the maximum instantaneous displacement envelope $y_{e\max}$ (measured by the vibrometer, and calculated on the basis of formula (15)) are growing with an increase in the cutting speed v_c. It confirms the fact that during the milling process, cutter displacement related to radial run-out is affected by centrifugal forces, which grow as the rotational speed (and thus cutting speed) increases. However, considerable values of error bars (especially for v_c =200 m/min) confirm that the cutter displacement envelope is also influenced by some random phenomena. From Fig. 8a it can be also seen that $y_{e\max}$ values calculated based on formula (15) correspond with the measured ones.

The average values of maximum instantaneous total displacement $y_{\max}$ are growing in the cutting speed v_c function(Fig. 8b). This phenomenon is related to an increase in the feed normal force F_{fN} within the function of the investigated cutting speeds (Fig. 8b). It can be deduced from formula (4) that the resulting force generated in the milling process is proportional to total cutter displacement. Total cutter displacement increase is an undesirable phenomenon because it contributes to an increase in surface location error (SLE).

www.czasopisma.pan.pl   PAN   www.journals.pan.pl
POLSKA AKADEMIA NAUK

S. Wojciechowski: MACHINED SURFACE ROUGHNESS INCLUDING CUTTER DISPLACEMENTS IN MILLING OF ...

Fig. 9 depicts the influence of cutting speed v_c on measured (using surface profilometer) and calculated (using formulas (2) and (3)) surface roughness parameters (Ra – Fig. 9a, Rz – Fig. 9b). As can be observed (Fig. 9), the cutting speed has a small influence on real surface roughness parameters Ra, Rz, which is confirmed by considerable values of error bars, as well as the low values of the correlation coefficients ($R^2 < 0.24$ for Ra and $R^2 < 0.37$ for Rz). Nevertheless, for the highest investigated cutting speed ($v_c = 500$ m/min), mean surface roughness parameters Ra and Rz were higher than those obtained for the lowest cutting speed ($v_c = 100$ m/min). This means that in the investigated range, measured surface roughness is insignificantly affected by the displacements induced by centrifugal forces.

According to the kinematic-geometric basic model, theoretical surface roughness height Rt_0 is scarcely 0.21 µm, on the other hand real and modeled surface roughness values are from 19 to 38 times higher. From Fig. 9 it can be seen that the developed surface roughness model including dynamic cutter displacements significantly increases the estimation accuracy of the surface roughness parameters $Ra(y_{emax})$, $Rz(y_{emax})$, in comparison with the theoretic basic model Rt_0. Both calculated and measured surface roughness Rz values are close to cutter displacement envelope values y_{emax} (see Fig. 8a). This means that during the process of finishing milling of hardened steel, the generated surface roughness is mainly affected by the cutter's radial run-out. This results from geometrical errors of the machine-collet-tool system. Nevertheless some discrepancies between measured and calculated surface roughness parameter values are found. The above-mentioned discrepancies are probably caused by simplifications assumed in the model (*e.g.* negligence of minimum uncut chip thickness problem), as well as some random phenomena occurring in surface roughness generation.
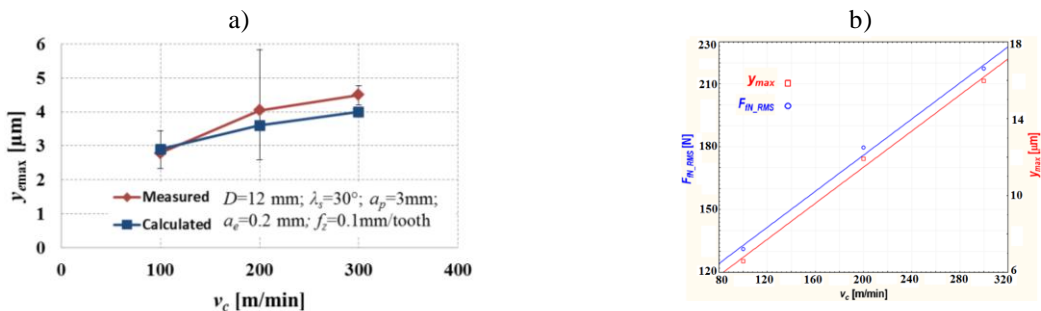

Fig. 8. a) maximum instantaneous displacement envelope y_{emax} per tool revolution in function of cutting speed v_c; b) maximum instantaneous total displacement y_{max} per each tooth and feed normal force F_{fN_RMS} in function of cutting speed v_c.
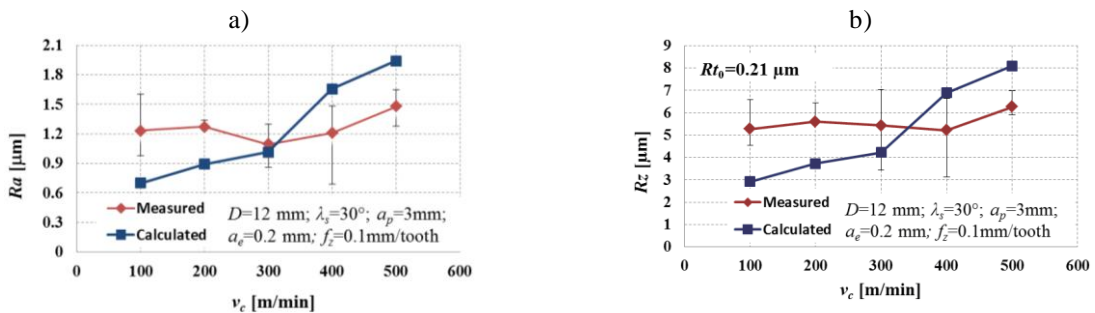

Fig. 9. a) surface roughness Ra in function of cutting speed v_c; b) surface roughness Rz in function of cutting speed v_c.

4. Conclusions

This paper investigated the surface roughness generated in cylindrical milling of hardened steel. A surface roughness model including cutter displacements was also developed.

As it is well known from the traditional kinematic-geometric model, surface roughness is affected by the f_z feed per tooth and tool diameter D values. However, the above-mentioned model is not including many important phenomena occurring in a cutting process as: cutter displacements, alterations of cutting edge shape, alterations of tooth immersion into the work piece along the cutting path or the influence of chip formation discontinuities on the surface texture.

The conducted research revealed that in the process of finishing milling of hardened steel, dynamic cutter displacement related to radial run-out is the crucial factor affecting machined surface roughness. This phenomenon induces the alterations of maximal instantaneous displacements per consecutive tooth, as well as the oscillations of maximal instantaneous force amplitude. Alterations of these instantaneous maximal displacements produce the envelope whose period is equal to the tool revolution time. Therefore surface roughness generated in the milling process is related to the feed per revolution value f instead of the feed per tooth f_z value (according to the kinematic-geometric basic model). It was also found that cutting speed has a slight influence on real surface roughness parameters Ra, Rz, which was confirmed by considerable values of error bars, as well as low values of correlation coefficients. This means that in the investigated range, measured surface roughness is mainly affected by the cutter's radial-run-out resulting from geometrical errors of the machine-collet-tool system instead of displacements induced by centrifugal forces.

The developed surface roughness model including dynamic cutter displacements significantly increases the estimation accuracy of the surface roughness parameters $Ra(y_{emax})$, $Rz(y_{emax})$, in comparison to theoretic basic model Rt_0.

References

[1] Wojciechowski, S., Twardowski, P. (2011). Machined surface roughness in the aspect of milling process dynamics. *13th International Conference on Metrology and Properties of Engineering Surfaces.* 12–15 April 2011 Twickenham Stadium, UK, 87-91.

[2] Wieczorowski, M. (2002). Future trends of surface morphology analysis. *Metrology and Measurement Systems,* 9(3), 221-234.

[3] Kawalec, M., Rybicki, M. (2003). Surface formation during face finish milling of hardened steels. *Archives of Mechanical Technology and Automation,* 23 (2), 61-66. (in Polish)

[4] Villaseñor, D., Morales-Menéndez, R., Rodrıguez, C. (2006). Neural networks and statistical based models for surface roughness prediction. *Proceedings of the 25th IASTED International Conference Modelling, Identification and Control*, Lanzarote, 326-331.

[5] Vivancos, J., Luis, C., Costa, L., Ortız, J., González, H. (2005). Analysis of factors affecting the high-speed side milling of hardened die steels. *Journal of Materials Processing Technology*, London, 696-701.

[6] Vivancos, J., Luis, C., Costa, L., Ortız, J. (2004). Optimal machining parameters selection in high speed milling of hardened steels for injection moulds. *Journal of Materials Processing Technology*, London, 1505-1512.

[7] Twardowski, P., Staniek, R., Wojciechowski, S. (2010). The Influence of High Speed Milling Dynamics on Surface Roughness of Hardened Steel. *Proceedings of 4th CIRP International Conference on High Performance Cutting*, Nagaragawa Convention Center, Gifu, Japan, 19-24.

[8] Wieczorowski, M., Twardowski, P., Wojciechowski, S., Mathia, T.G. (2010). Some Aspects of Hardened Steel HSM. *Process Dynamics and Modeling in Relation to Surface Roughness, Proceedings of the 2nd Int. Conf. on Surface Metrology*, Worcester, ISBN 978-1-4507-4290-0, 102-112.

[9] Twardowski, P. (2011). Surface roughness analysis in milling of tungsten carbide with CBN cutters. *Metrology and Measurement Systems*, 18(1), 105-114.

[10]   El-Wardany, T.I., Kishawy, H.A., Elbestawi M.A. (2000). Surface integrity of die material in high speed hard machining, Part 1: Micrographical analysis. *Transactions of the ASME, Journal of Manufacturing Science and Engineering*, 122, 620-631.

[11]   Smith, S., Winfough, W.R., Halley, J. (1998). The effect of tool length on stable metal removal rate in high speed milling. *Annals of the CIRP*, 47(1), 307-310.

[12]   Tlusty, J., Smith, S. (1997). Current Trends in High-Speed Machining. *Journal of Manufacturing Science and Engineering*, 119, 664-666.

[13]   Antoniadis, A., Savakis, C., Bilalis, N., Balouktsis, A. (2003). Prediction of surface topomorphy and roughness in ball-end milling. *International Journal of Advanced Manufacturing Technology*, 21, 965-971.

[14]   Jung, T.S., Yang, M.Y., Lee K.J. (2005). A new approach to analysing machined surfaces by ball-end milling, part II: Roughness prediction and experimental verification. *International Journal of Advanced Manufacturing Technology*, 25, 841-849.

[15]   Lou, M., Chen, J., Li, C. (1998). Surface roughness prediction technique for CNC end-milling. *Journal of Industrial Technology*, 15(1), 1-6.

[16]   Weck, M., Schmidt, M. (1986). A new method for determining geometric accuracy in the axis of movement of machine tools. *Precision Engineering*, 8(2).

[17]   Heisel, U., Feinauer, A. (1999). Dynamic influence on workpiece quality in high speed milling. *Annals of the CIRP*, 48(1), 321.

[18]   Lopez, L.N., Lamikiz, A., Sanchez, J.A., Salgado, M.A. (2004). Effects of tool deflection in high-speed milling of inclined surfaces. *International Journal of Advanced Manufacturing Technology*, 24, 621-631.

[19]   Surmann, T., Biermann, D. (2008). The effect of tool vibration on the flank surface created by peripheral milling. *Annals of the CIRP*, 57, 375-378.

[20]   Surmann, T., Enk, D. (2007). Simulation of milling tool vibration trajectories along changing engagement conditions. *International Journal of Machine Tools & Manufacture*, 47, 1442-1448.

[21]   Tlusty, J., Smith, S., Winfough, W.R. (1996). Techniques for the use of long slender end mills in high-speed milling. *Annals of the CIRP*, 45(1), 393-396.

[22]   Toh, C.K. (2004). Vibration analysis in high speed rough and finish milling of hardened steel. *Journal of Sound and Vibration*, 278, 101-115.

[23]   Twardowski, P. (2008). Influence of dynamics process milling of hardened steel on machined surface roughness in HSM conditions. *Archives of Mechanical Technnology and Automation,* 28 (2), 111-115. (in Polish)

[24]   Insperger, T., Gradisek, J., Kalveram, M., Stepan, G., Winert, K., Govekar, E. (2006). Machine Tool Chatter and Surface Location Error in Milling Processes. *Journal of Manufacturing Science and Engineering*, 128, 913-920.

[25]   Liu, X., Cheng, K. (2005). Modelling the machining dynamics of peripheral milling. *International Journal of Machine Tools & Manufacture* 45, 1301-1320.

[26]   Seguy, S., Dessein, G., Arnaud, L. (2008). Surface roughness variation of thin wall milling, related to modal interactions. *International Journal of Machine Tools & Manufacture* 48, 261-274.

[27]   Paris, H., Peigne, G. Mayer, R. (2004). Surface shape prediction in high speed milling. *International Journal of Machine Tools & Manufacture* 44, 1567-1576.

[28]   Omar, O.E.E.K., El-Wardany, T., Ng, E., Elbestawi, M.A. (2007). An improved cutting force and surface topography prediction model in end milling. *International Journal of Machine Tools & Manufacture*, 47, 1263-1275.

[29]   Schmitz, T.L., Couey, J., Marsh, E., Mauntler, N., Hughes, D. (2007). Runout effects in milling: Surface finish, surface location error, and stability. *International Journal of Machine Tools & Manufacture* 47, 841-851.